



HAL
open science

Optical anisotropy in the VUV range: experimental studies and dielectric constants of monoclinic GaTe

G. Levêque, C.G. Olson, D.W. Lynch

► **To cite this version:**

G. Levêque, C.G. Olson, D.W. Lynch. Optical anisotropy in the VUV range: experimental studies and dielectric constants of monoclinic GaTe. *Journal de Physique*, 1984, 45 (10), pp.1699-1706. 10.1051/jphys:0198400450100169900 . jpa-00209911

HAL Id: jpa-00209911

<https://hal.science/jpa-00209911>

Submitted on 4 Feb 2008

HAL is a multi-disciplinary open access archive for the deposit and dissemination of scientific research documents, whether they are published or not. The documents may come from teaching and research institutions in France or abroad, or from public or private research centers.

L'archive ouverte pluridisciplinaire **HAL**, est destinée au dépôt et à la diffusion de documents scientifiques de niveau recherche, publiés ou non, émanant des établissements d'enseignement et de recherche français ou étrangers, des laboratoires publics ou privés.

Classification
 Physics Abstracts
 78.40

Optical anisotropy in the VUV range : experimental studies and dielectric constants of monoclinic GaTe

G. Levêque (*), C. G. Olson and D. W. Lynch

Ames Laboratory and Department of Physics, Iowa State University, Ames, Iowa 50011,
 and Synchrotron Radiation Center, University of Wisconsin-Madison-Stoughton, Wisconsin 53589, U.S.A.

(Reçu le 12 janvier 1984, révisé le 21 mai, accepté le 12 juin 1984)

Résumé. — La réflectance de GaTe entre 2,5 et 26 eV, sous incidence normale et oblique, a été mesurée à l'aide d'un rayonnement synchrotron polarisé. Nous en avons déduit 3 indices de réfraction complexes relatifs aux 3 directions cristallographiques, en utilisant une nouvelle méthode de calcul, incorporant les relations de Kramers-Kronig. Il se vérifie que les transitions électroniques dans le domaine des 20 eV, à partir des niveaux 3d Ga, sont fortement localisées près des atomes de gallium. Certaines transitions à partir de la bande de valence apparaissent aussi plus ou moins localisées.

Abstract. — Normal and oblique incidence reflectances of GaTe have been measured in the 2.5 to 26 eV range using polarized synchrotron radiation. We have deduced 3 complex refractive indices, relative to 3 different crystallographic directions by means of a new method consistent with the Kramers-Kronig relations. We have verified that the electronic transitions in the 20 eV region, from the 3d Ga levels, are strongly localized near gallium atoms. Some transitions from the valence band also appear localized.

1. Introduction.

Layered compounds are highly anisotropic materials because of their atomic structures, with plane layers weakly bonded to each other. For many of these compounds, the individual layers have a hexagonal bidimensional lattice and all directions in the plane of the layers are optically equivalent. These crystals, like GaS or GaSe, therefore have uniaxial properties with the optical axis normal to the planes. Some other compounds, like GaTe, have layers with a rectangular lattice and are consequently biaxial in nature.

Optically flat and clean surfaces cannot be obtained with layered crystals except for the cleavage plane. The determination of the complex refractive index tensor requires measurements of reflectance at normal and oblique incidence on the cleaved surface. For oblique reflectance measurements with lineary polarized beams, four configurations can be distinguished, depending on the relative position of the electric vector, the incidence plane and the crystal. Configurations for $R_{E\parallel a}^s$, $R_{E\parallel b}^s$, $R_{E\perp a}^p$ and $R_{E\perp b}^p$ are shown schematically in figure 1, s or p indicate that the electric vector E is normal to, or in, the incidence plane; a

and b are orthogonal vectors in the surface of the crystal.

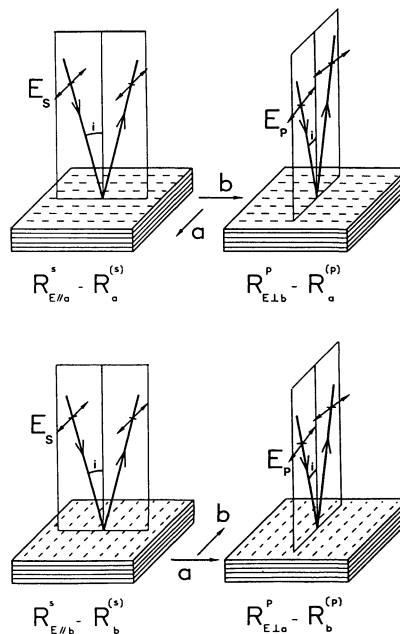


Fig. 1. — Different configurations for reflectance measurements on a monoclinic layered compound with a lineary polarized beam (left notation) or in partly polarized beam (right notation).

(*) Current and permanent address : Laboratoire de Spectroscopie II, Université des Sciences et Techniques du Languedoc, 34060 Montpellier, France.

A classical method [1, 2] for deducing the ordinary and extraordinary refractive indices of a uniaxial layered material from experimental reflectances is to adjust the four independent parameters (n_o , k_o , n_e , k_e) in order to find the best possible fit with the experimental $R(\theta)$ curves. This method has been applied in the VUV range [2] but meets some difficulties for the following reasons :

— fully polarized beams are not available in this range and even synchrotron radiation beams are only partly polarized. In this case, the degree of polarization needs to be introduced as a supplementary parameter

— important errors [3] in the results can arise from very small experimental errors because the data depend on several independent parameters. This error enhancement is particularly conspicuous for the extraordinary index which is less strongly coupled with reflectance than the ordinary index

— the various $\tilde{N}(h\omega)$ obtained are not consistent with the Kramers-Kronig relation, which is a serious problem, regarding the meaning of the deduced structures.

We have shown [4] that some of these problems can be partly resolved by including KK consistency as a supplementary condition during the deduction of the different parameters from reflectance data. We will demonstrate here that one can keep the Kramers-Kronig consistency also in the more complicated case of some biaxial layered compounds.

2. Mathematical framework.

The compound GaTe crystallizes in a monoclinic C_{2h} form [5] with the cleavage plane containing the second-order axis b taken as the y coordinate ; x and z axes are set tangential and normal to the cleavage plane. In this configuration the dielectric tensor $\bar{\epsilon}$ is expressed as

$$\bar{\epsilon} = \begin{vmatrix} \epsilon_{xx}(\omega) & 0 & \epsilon_{xz}(\omega) \\ 0 & \epsilon_{yy}(\omega) & 0 \\ \epsilon_{xz}(\omega) & 0 & \epsilon_{zz}(\omega) \end{vmatrix}$$

where all components are complex.

In general monoclinic crystals, it will not be possible to bring the tensor into diagonal form with axes fixed in the crystal, and only waves with $E \parallel y$ correspond to pure transverse waves in the medium [6]. Only the $R_{E \parallel b}^s$ configuration corresponds to this case and the reflectance is then formally the same as for isotropic medium :

$$R_{E \parallel b}^s = \left| \frac{\cos i - \sqrt{\epsilon_{yy} - \sin^2 i}}{\cos i + \sqrt{\epsilon_{yy} - \sin^2 i}} \right|^2.$$

For the configuration $R_{E \perp b}^p$ the incidence plane coincides with the symmetry plane of the crystal. In

this case, the wave is refracted in the incidence plane and is linearly polarized. The reflectance in this case is given in reference [6] :

$$R_{E \perp b}^p = \left| \frac{(\sqrt{\epsilon_{xx} \epsilon_{zz} - \epsilon_{xz}^2}) \cos i - \sqrt{\epsilon_{zz} - \sin^2 i}}{(\sqrt{\epsilon_{xx} \epsilon_{zz} - \epsilon_{xz}^2}) \cos i + \sqrt{\epsilon_{zz} - \sin^2 i}} \right|^2.$$

The other two configurations are more complicated as the reflected and refracted waves are elliptically polarized. To our knowledge no formulation is available for the reflectances $R_{E \parallel a}^s$ and $R_{E \perp a}^p$ (the general expressions given by Berek [7] cannot be applied here). The derivation of the four components of $\epsilon(\omega)$ would seem then to be difficult from reflectance data relative to the unique accessible surface of this biaxial layered compound.

We have tried to reduce the complexity of the problem by making some realistic approximations. In the low energy range, layered material show a great anisotropy due to the bidimensional character of the structure [8]. The optical properties depend mainly upon the orientation of the electric field relative to the layer plane. The real and the imaginary part of $\bar{\epsilon}$ can then be diagonalized in a coordinate system uvv only slightly tilted relative to the plane xy of the layer as in the left side of figure 2. If the tilt angle α is small, the index ellipsoid of this monoclinic crystal can be reasonably approximated by the ellipsoid corresponding to an orthorhombic crystal (dotted lines on Fig. 2).

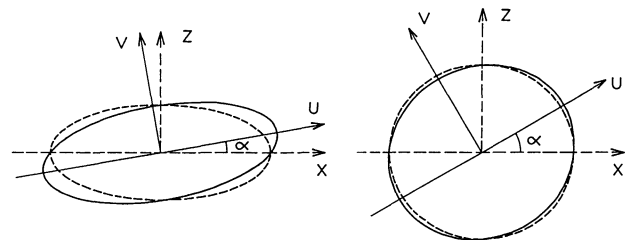


Fig. 2. — Index ellipsoid trace in the xz plane. Left side : nearly bidimensional case, right side : nearly isotropic case.

On the other hand, in the range where the optical anisotropy is small, the index ellipsoid is not far from a sphere (right side of Fig. 2). There also an orthorhombic ellipsoid provides a valuable approximation. We have then chosen to treat our data with orthorhombic reflectance formulae, because they are the most complete general expressions usable for our four configurations and because they probably give a good approximation of the true expressions.

The expressions for reflectance from the xy plane of an orthorhombic material with principal axes xyz are formally the same for (010) and (100) as a plane of incidence and can be derived from reference [6] by taking $\epsilon_{xz} = 0$:

$$R_{E \parallel a}^s = \left| \frac{\cos i - \sqrt{\epsilon_x - \sin^2 i}}{\cos i + \sqrt{\epsilon_x - \sin^2 i}} \right|^2$$

$$R_{E\parallel b}^s = \left| \frac{\cos i - \sqrt{\varepsilon_y - \sin^2 i}}{\cos i + \sqrt{\varepsilon_y - \sin^2 i}} \right|^2$$

$$R_{E\perp a}^p = \left| \frac{(\varepsilon_y \varepsilon_z)^{1/2} \cos i - \sqrt{\varepsilon_z - \sin^2 i}}{(\varepsilon_y \varepsilon_z)^{1/2} \cos i + \sqrt{\varepsilon_z - \sin^2 i}} \right|^2$$

$$R_{E\perp b}^p = \left| \frac{(\varepsilon_x \varepsilon_z)^{1/2} \cos i - \sqrt{\varepsilon_z - \sin^2 i}}{(\varepsilon_x \varepsilon_z)^{1/2} \cos i + \sqrt{\varepsilon_z - \sin^2 i}} \right|^2$$

and for partly polarized beams with polarization factor P :

$$P = \frac{I^s - I^p}{I^s + I^p}$$

$$R_a = \frac{1}{2} [R_{E\parallel a}^s(1 + P) + R_{E\perp a}^p(1 - P)]$$

$$R_b = \frac{1}{2} [R_{E\parallel b}^s(1 + P) + R_{E\perp b}^p(1 - P)].$$

To extract the different complex dielectric constants and the polarization factor from the experimental data R_a and R_b , we have used an iterative method, each iteration having two steps. The first step evaluates the different corrective terms to be applied to the preceding values of the 7 parameters ($\tilde{\varepsilon}_x, \tilde{\varepsilon}_y, \tilde{\varepsilon}_z, P$) to find the best fit with the experimental data at each photon energy. The second step restores Kramers-Kronig consistency. As the second step partly cancels the aim of the first one, a careful choice of mathematical method has been made in order to give good convergence of all parameters.

2.1 EVALUATION OF CORRECTIVE TERMS. — The set of experimental curves is composed of J reflectance values at each photon energy, for different configurations and incidence angles. As in the least squares method, we used the sum of the relative errors :

$$S = \sum_{j=1 \text{ to } J} \left(\frac{R_{\text{exp}}^j - R^j}{R^j} \right)^2$$

and its derivatives in the vectorial space of the 7 parameters. Actually, it appears easier to work with the refractive indexes $\tilde{N} = \tilde{\varepsilon}^{1/2}$ in the calculated $R^j(n_x, k_x, n_y, k_y, n_z, k_z, P)$.

In some least squares methods, the corrective terms are set proportional to the components of the gradient of S . This procedure is not convenient in our case because the partial derivatives $\frac{\partial S}{\partial n_z}$ and $\frac{\partial S}{\partial k_z}$ are much smaller than the other derivatives in the 2 to 15 eV range [7], which gives no significant correction to the corresponding parameters n_z and k_z .

We have avoided this difficulty by calculating corrective terms which minimize separately the S function. The independent corrective terms that mini-

mize S are determined by allowing a linear dependence of R^j in function of Δn_x :

$$R^j = R_0^j + \frac{\partial R^j}{\partial n_x} \Delta n_x$$

which gives

$$S = \sum_j \left(\frac{R_{\text{exp}}^j - R_0^j - \frac{\partial R^j}{\partial n_x} \Delta n_x}{R_0^j} \right)^2.$$

Resolving the linear equation $\frac{dS}{d\Delta n_x} = 0$ permits the determination of Δn_x :

$$\Delta n_x = \frac{\sum_j \left(\frac{R_{\text{exp}}^j - R_0^j}{(R_0^j)^2} \right) \frac{\partial R^j}{\partial n_x}}{\sum_j \left(\frac{1}{R_0^j} \frac{\partial R^j}{\partial n_x} \right)^2}.$$

The other six parameters are derived in the same manner. In order to keep the modulus of the applied correction $\delta\tilde{N} = \delta n + i\delta k$ as small as possible, we have combined the two terms of each group to obtain the modified terms.

$$\delta n_x = \frac{\Delta n_x (\Delta k_x)^2}{(\Delta n_x)^2 + (\Delta k_x)^2} \quad \text{and} \quad \delta k_x = \frac{\Delta k_x (\Delta n_x)^2}{(\Delta n_x)^2 + (\Delta k_x)^2}$$

as shown in figure 3. $\delta\tilde{N}_x, \delta\tilde{N}_y$ and $\delta\tilde{N}_z$ are calculated separately with this method. The procedure of an exact correction of 4 parameters ($\tilde{N}_x, \tilde{N}_y, \tilde{N}_z, P$) leads to an overcorrection when applied simultaneously, but is better than the correction along the gradient which is not effective for \tilde{N}_z .

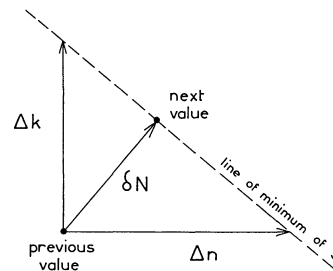


Fig. 3. — Different \tilde{N} corrections in the n_x, n_y plane ($\delta\tilde{N} = \delta n_x + i\delta k_x$).

2.2 KRAMERS-KRONIG CORRECTION. — The δn and δk values deduced from the preceding section are not consistent with the Kramers-Kronig relation, neither are the n_1 and k_1 values

$$n_1 = n_0 + \delta n$$

$$k_1 = k_0 + \delta k$$

obtained after the correction of the values n_0 and k_0 from the preceding iteration. In order to preserve the

formal symmetry between n and k , we calculate the final terms of the iteration n_2 and k_2 as :

$$n_2(\omega) = \frac{1}{2} \left[n_1(\omega) + 1 + \frac{2}{\pi} \int_0^\infty \frac{\omega' k_1(\omega') d\omega'}{\omega'^2 - \omega^2} \right]$$

$$k_2(\omega) = \frac{1}{2} \left[k_1(\omega) - \frac{2\omega}{\pi} \int_0^\infty \frac{n_1(\omega') d\omega'}{\omega'^2 - \omega^2} \right].$$

which are Kramers-Kronig consistent.

This method allows extrapolations using experimental absorption data in a much easier manner than that of reference [9]. In the range where the reflectances are not known, δn and δk cannot be calculated as in § 2.1, we have used instead the following terms :

$$\delta n = 0, \quad \delta k = \frac{c}{2\omega} \mu_{\text{exp}} - k_{\text{calc}}$$

deduced from the experimental absorption coefficient $\mu = \frac{2\omega}{c} k$. This procedure assures that the calculated n, k are fully consistent with the reflectances in the measured range, with the transmission data in the transparence region, near and below the gap, and with the atomic cross-sections in the high energy region.

3. Experimental device and results.

The procedure described above has been applied to experimental reflectances in the 2.5 to 27 eV range obtained at the Synchrotron Radiation Center, University of Wisconsin, Madison. With an apparatus already described [10], we have measured 8 reflectance curves reported in figures 4 and 5 at two angles of incidence for each of the four configurations of figure 1. Several diaphragms and a chopping filter eliminate most of the scattered light and the long wavelength light diffused by the grating. But as the

geometry of the system changes slightly in function of the angle of incidence and because the detector has a non uniform sensivity, the experimental errors on the absolute values of R may reach $\Delta R/R = 10\%$. However the relative variations of R in a spectrum are measured much more accurately.

The angular aperture of the incident beam was 0.5° but as the surface of the sample was not perfectly flat we have considered an uncertainty of $\pm 1^\circ$ for the angle of incidence. The (s) and (p) configurations were obtained by rotating the entire experimental chamber around the beam axis. As GaTe had proved to be very sensitive to air exposure [9] the samples were cleaved in vacuum just before the experiments.

Previous measurements are reported on figure 4. The curve from reference [10] represents the data obtained with unpolarized beam on a much smaller GaTe crystal. The better optical quality of our present sample explains the differences in the measured reflectances. The spectrum of reference [11] has been adjusted to an arbitrary absolute value because the original data are in relative units.

Ten computer iterations were necessary to obtain stable values of the different parameters. In order to test if the curves obtained do not present spurious structures produced by calculation effects, we have performed the same calculation after introducing some scale factors on the experimental curves. We have shown that experimental errors give errors of the same order of magnitude in the different computed parameters, but no extraneous structures.

We have noted that the uncertainty in the $\tilde{\epsilon}_z$ value is at least twice as large as those produced in the $\tilde{\epsilon}_x$ and $\tilde{\epsilon}_y$ values. This phenomenon appears because the derivatives of R with respect to n_z and k_z are much smaller than the other derivatives. This effect is so important in the low energy range that computed ϵ_z values below 4 eV are meaningless.

Figure 6 presents reflectance curves deduced from the calculated $\tilde{\epsilon}$ values by $R^n = |(1 - \tilde{\epsilon}^{1/2}) / (1 + \tilde{\epsilon}^{1/2})|^2$,

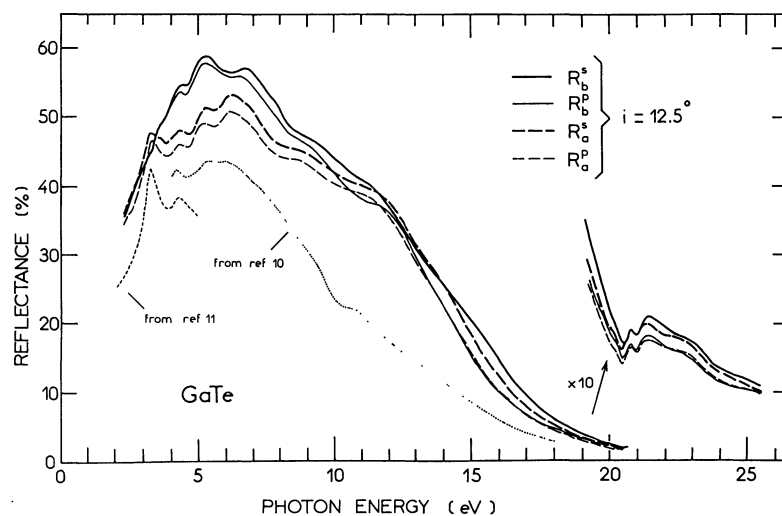


Fig. 4. — Normal incidence reflectances on GaTe.

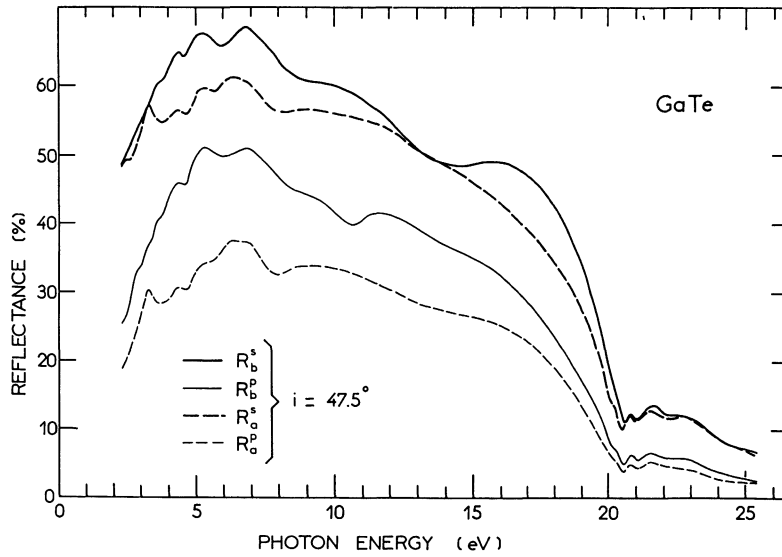


Fig. 5. — Oblique incidence reflectances on GaTe.

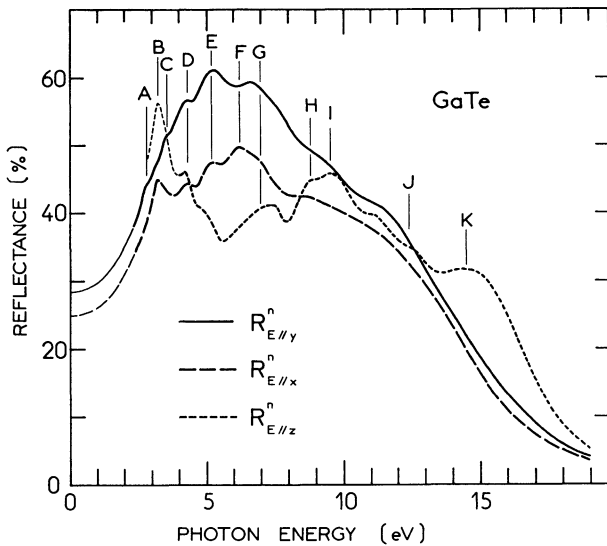


Fig. 6. — Computed reflectance curves corresponding to the three directions of the field, deduced from ϵ_x , ϵ_y and ϵ_z . Thinner lines on the low energy part of the spectrum indicate less accurate curves, because of extrapolations on $R_{E||x}$ and $R_{E||y}$ and great uncertainty in $R_{E||z}$.

which are easier to compare with experimental reflectance curves. The curves $R_{E||x}^n$ and $R_{E||y}^n$ represent the normal incidence reflectance on the cleavage plane (001) and $R_{E||z}^n$ represents normal incidence on a hypothetical (010) edge of the crystal.

In figure 7, we have plotted the imaginary part of $\tilde{\epsilon}$ for the three different orientations of the electric vector, in the energy range of transitions from 3d Ga deep levels.

The polarization factor P issued from our calculation is plotted on figure 8. We have reported for comparison the theoretical polarization factor for the

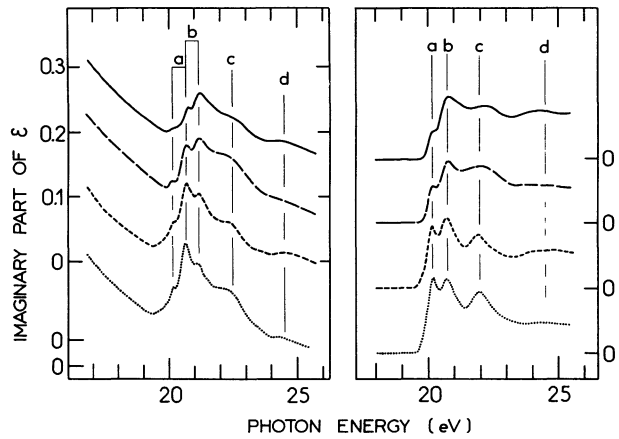


Fig. 7. — Imaginary part of the dielectric constant — $\epsilon_y = \epsilon_{\perp}$, — ϵ_x , - - - ϵ_z , ... $\epsilon_x + \epsilon_z - \epsilon_y = \epsilon_{\parallel}$, left side : raw data from calculation, right side : curves obtained by subtraction of a continuous background and by deconvolution of the spin-orbit structure of Ga.

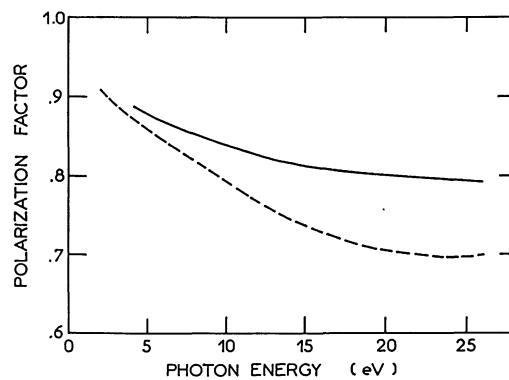


Fig. 8. — Polarization factor. Heavy line : theoretical factor for tantalus I emission, dotted line : values used in our calculation.

tantalus I synchrotron emission in a 4 mrad aperture. The polarization of the incident beam may be slightly different because of the grating and the focusing mirror before the monochromator. Actually our P values does not constitute a true measurement of the polarization factor as the P parameter may correct and include some of the errors in the reflectance absolute values.

4. Discussion.

The anisotropy of the spectra appears clearly on the figures 6 and 7. But the spectrum $R_{E\parallel z}$ does not lie very separate from the two other spectra. In the studied optical range, the GaTe crystal exhibits a definite three dimensional character, the difference between \tilde{N}_x , \tilde{N}_y and \tilde{N}_z being of the same order of magnitude. It can be concluded that, for biaxial GaTe, the layered structure is not determinant for the optical properties. In this case the approximations in reflectance expressions (the neglect of the ε_{xz} term) appear less justified and a more complete experiment and data reduction would be interesting.

The electronic structure of GaTe seems poorly understood compared to those of GaSe and GaS. This arises probably from the more complicated crystal structure of GaTe and the necessity of treating it relativistically which have prevented the development of band structure calculations. On the other hand, the few photoemission spectra available for GaTe [13, 14] have not given a coherent view of the structure of the valence band. Under these conditions it seems difficult to discuss the origin of the different structures observed in our reflectance curves.

Because of its special atomic arrangement, GaTe gives however an unique tool for testing the effects of atomic orientation on the optical properties. Let us first describe the atomic structure of this compound as it appears in reference [5].

A section of the crystal perpendicular to the b axis is reported in the upper figure 9. The unit cell represented in the figure extends in one layer and, according to the symmetry of the crystal, includes 3 different gallium atoms and 3 different tellurium atoms, noted Ga 1, 2, 3 and Te 1, 2, 3 respectively. It can be noted that each gallium atom is bounded to 3 tellurium atoms and to another gallium atom in nearly tetrahedral directions. On the other hand the tellurium atoms appear in nearly equivalent positions, with the Ga-Te bondings in tetrahedral directions, the fourth direction being unoccupied. In conclusion, each atom seems to have a ternary symmetric neighbourhood with the axis of symmetry along the x direction for Ga 1 and along the z direction for all others.

In the case of optical transitions with pure atomic character, the selection rules depend on the orientation of the electric field E relative to the axis of symmetry of the electronic structure. If we note χ_{\perp} and χ_{\parallel} the response of one atom to excitation with E normal

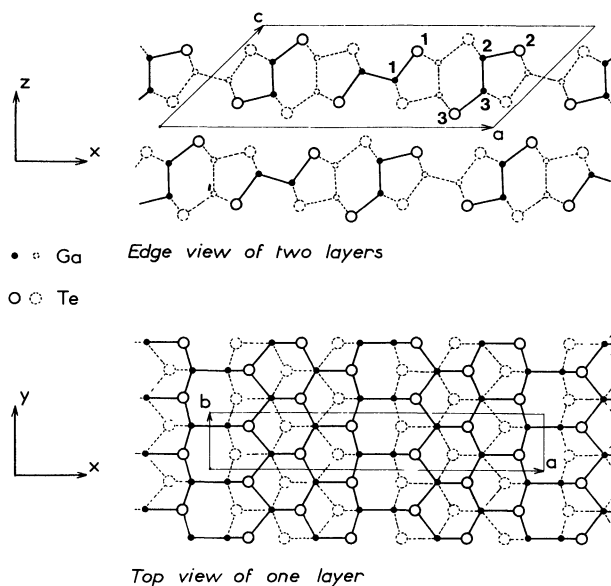


Fig. 9. — Atomic arrangement in GaTe.

or parallel to the axis of symmetry of the structure, the resultant response of the medium will be :

$$\begin{aligned}\chi_{E\parallel x} &= \chi_{\parallel}^{\text{Ga}1} + \chi_{\perp}^{\text{Ga}2} + \chi_{\perp}^{\text{Ga}3} + \chi_{\perp}^{\text{Te}1} + \chi_{\perp}^{\text{Te}2} + \chi_{\perp}^{\text{Te}3} \\ &= 2 \chi_{\perp}^{\text{Ga}} + \chi_{\parallel}^{\text{Ga}} + 3 \chi_{\perp}^{\text{Te}} \\ \chi_{E\parallel y} &= \chi_{\perp}^{\text{Ga}1} + \chi_{\perp}^{\text{Ga}2} + \chi_{\perp}^{\text{Ga}3} + \chi_{\perp}^{\text{Te}1} + \chi_{\perp}^{\text{Te}2} + \chi_{\perp}^{\text{Te}3} \\ &= 3 \chi_{\perp}^{\text{Ga}} + 3 \chi_{\parallel}^{\text{Te}} \\ \chi_{E\parallel z} &= \chi_{\perp}^{\text{Ga}1} + \chi_{\parallel}^{\text{Ga}2} + \chi_{\parallel}^{\text{Ga}3} + \chi_{\parallel}^{\text{Te}1} + \chi_{\parallel}^{\text{Te}2} + \chi_{\parallel}^{\text{Te}3} \\ &= \chi_{\perp}^{\text{Ga}} + 2 \chi_{\parallel}^{\text{Ga}} + 3 \chi_{\parallel}^{\text{Te}}.\end{aligned}$$

It is worth noting that these relations are only approximate because the electronic structure of each atom has not exactly a 3 fold symmetry around the x or z axis, but only a mirror plane parallel to xy , like the crystal.

Let us now try to apply these considerations to the optical properties of GaTe. We will focus our discussion on the reflectance spectrum in the low energy range (2-15 eV) and on the imaginary part of dielectric constant in the 18 to 27 eV region (we ignore the non-linear dependence of R on the dielectric properties of the material which has a small effect in comparison with the other approximations made before).

The structures in the high energy range are due to transitions from the Ga3d deep level into conduction states. According to the preceding equations, we expect to have

$$\varepsilon_x \cong 1/2(\varepsilon_y + \varepsilon_z).$$

The left side of figure 7 shows that this equation is verified to a good approximation, indicating that the optical properties in this energy range behave like atomic phenomena. Pure ε_{\perp} and ε_{\parallel} deduced from above :

$$\begin{aligned}\varepsilon_{\perp} &= \varepsilon_y \\ \varepsilon_{\parallel} &= \varepsilon_x + \varepsilon_z - \varepsilon_y\end{aligned}$$

are presented in the same figure.

	A	B	C	D	E	F	G	H	I	J	K
$R_{E\parallel y}$	2.85		<u>3.55</u>	<u>4.35</u>	<u>5.3</u>		6.75	9.4		11.6	
$R_{E\parallel x}$		3.25		4.35	5.2	6.2	7.0	8.75			
$E_{E\parallel z}$		<u>3.30</u>		4.25	5.1		7.3	<u>8.8</u>	<u>9.5</u>	11.2	<u>14.5</u>
localization		Ga		Ga	Ga		Ga	Te			Te

transition from Ga3d levels

$\epsilon_{\perp} = \epsilon_y$	19.9	20.2	20.75	<u>21.25</u>	22.8	24.4	
ϵ_x	19.9	20.15	20.7	21.2	22.4		
ϵ_z	19.4	20.2	20.7	21.2	22.4	24.5	
ϵ_{\parallel}	19.4	<u>20.2</u>	<u>20.7</u>	21.15	22.25	24.5	
	threshold				c	d	

Table I. — Energy in eV of the different structures in R and ϵ_2 . The strongest transitions are underlined.

As some structures appear to be separated by 0.5 eV, which is close to the value of the spin-orbit splitting of Ga3d levels of gallium (0.46 eV in pure Ga [15]), we have separated by deconvolution the spectra relative to the Ga3d 5/2 component from those relative to the Ga 3/2 and reported the first on the right part of the figure 7.

It appears that structures a and c show strong anisotropy while b and d seem more independent of the excitation orientation.

The problem is more complex in the low energy side of the spectrum where both gallium and tellurium orbitals contribute to less localized transitions. A first classification can be made between transitions localized near Ga or Te atoms by using the following rule deduced from the preceding relations :

- for transitions near Ga atoms : $R_{E\parallel x} = \frac{1}{2} \times (R_{E\parallel y} + R_{E\parallel z})$
- for transitions near Te atoms : $R_{E\parallel x} = R_{E\parallel y} \neq R_{E\parallel z}$.

It can be seen in figure 6 that structures B, D, E and G behave as the first type of transition, localized near or between gallium atoms. The transition corresponding to structures H and I seem rather localized near the tellurium atoms. The structures like A, C and F, which appear only in one spectrum are not identifiable by this method. The energetic position of these different structures are listed in table I.

5. Conclusion.

This work allows two different remarks. Firstly, we have been able to deduce three different dielectric constants of a biaxial material only from reflectance measurements on the cleavage surface of the crystal. Our method appears easy to use because it needs only 8 reflectance curves and is especially interesting because it gives results consistent with the Kramers-Kronig relations.

It should be noted however that our method is not free of some systematic errors because we have neglected the ϵ_{xz} term of the dielectric tensor.

Secondly, the particular arrangement of atomic bonds in GaTe has permitted us to verify the strongly localized character of the transitions from Ga3d deep level which appear nearly as atomic transitions. In the same manner, we have deduced probable localization for transitions from the valence band to the conduction band, which may be useful for comparison with further calculations or photoemission experiments.

Acknowledgments.

The large gallium telluride monocrystals used in this study were kindly supplied by A. Kuhn and A. Chevy, Laboratoire de Luminescence II, Université de Paris VI.

This work was supported by the U.S. Department

of Energy under Contract n° W-7405-Eng-82, Division of Materials Sciences Budget code Ak-01-02-02. It was carried out at the Synchrotron Radiation Center (SRC) of the Physical Sciences Laboratory of the University of Wisconsin-Madison. The storage

ring was operated under National Science Foundation Contract n° DMR-77-21888. G. L. wishes to thank the SRC for support and for making available the facilities with the help of which this work was carried out.

References

- [1] BERMAN, M., KERCHNER, H. R. and ERGUN, S., *J. Opt. Soc. Amer.* **60** (1970) 646.
- [2] THOMAS, J., LEMONNIER, J. C. and ROBIN, S., *Optica Acta* **19** (1972) 983.
- [3] HUNTER, W. R., *J. Opt. Soc. Amer.* **55** (1965) 1197.
- [4] LEVEQUE, G., BERTRAND, Y. and ROBIN-KANDARE, S., *Solid State Commun* **38** (1981) 759.
- [5] JULIEN-POUZOL, M., TAULMES, S., GUITTARD, M. and ALAPINI, F., *Acta Cryst.* **B 35** (1979) 2848.
- [6] KOCH, E. E., OTTO, A. and KLIEWER, K. L., *Chem. Phys.* **3** (1974) 362.
- [7] BERCK, M., *Z. Kristallogr.* **76** (1931) 396.
- [8] EVANS, B. L., *Optical Properties of layer compounds.* Physics and Chem. of Materials with Layered Structure (D. Reidel Pub. Comp. Dordrecht Holland) 1976, vol. 4, p. 1.
- [9] LEVFOUR, G. Thesis Montpellier 1979 unpublished
- [10] LEVEQUE, G., *J. Phys. C* **10** (1977) 4877.
- [11] BELLE, M. L. and GASANOVA, N. A., *Opt. Spectrosc.* **18** (1965) 412.
- [12] OLSON, C. G. and LYNCH, D. W., *Phys. Rev.* **B 9** (1974) 3159.
- [13] THOMAS, J., ADAMS, J., WILLIAMS, R. H. and BARBER, M., *J. Chem. Soc. Faraday Trans II* **5** (1972) 755.
- [14] WILLIAMS, R. H., MCGOVERN, I. T., MURRAY, R. B. and HOWELLS, M., *Phys. Status Solid.* **73b** (1976) 307.
- [15] EJIRI, A., SUGARAWA, F., OSUKI, H. and HIRANO, M., *Proc. Int. Conf. VUV V Montpellier* p. 25 (1977).